J. Fluid Mech. (2001), *vol.* 449, *pp.* 373–393.
DOI: 10.1017/S0022112001006401 Printed in the United Kingdom

On local boundary-layer receptivity to vortical disturbances in the free stream

By XUESONG WU

Department of Mathematics, Imperial College, 180 Queens Gate, London SW7 2BZ, UK

(Received 8 March 2001 and in revised form 19 July 2001)

Prompted by the recent experiments of Dietz (1999) on boundary-layer receptivity due to a local roughness interacting with a vortical disturbance in the free stream, this paper undertakes to present a second-order asymptotic theory based on the triple-deck formulation. The asymptotic approach allows us to treat vortical perturbations with a fairly general vertical distribution, and confirms Dietz's conclusion that for the convecting periodic wake in his experiments, the receptivity is independent of its vertical structure and can be fully characterized by its slip velocity at the edge of the boundary layer. As in the case of distributed vortical receptivity, dominant interactions that generate Tollmien–Schlichting waves take place in the upper deck as well as in the so-called edge layer centred at the outer reach of the boundary layer. The initial amplitude of the excited Tollmien–Schlichting wave is determined to $O(R^{-1/8})$ accuracy, where R is the global Reynolds number. An appropriate superposition formula is derived for the case of multiple roughness elements. A comprehensive comparison is made with Dietz's experimental data, and an excellent quantitative agreement has been found for the first time, thereby resolving some uncertainties about this receptivity mechanism.

1. Introduction

There has been considerable interest in understanding the boundary-layer receptivity, i.e. the process by which the external disturbances present in the environment produce a substantial response in the boundary layer (Morkovin 1969; Reshotko 1976). Of particular concern is how the unsteady free-stream disturbances generate Tollmien–Schlichting (T-S) instability waves. In a uniform incompressible free stream, a general unsteady small-amplitude perturbation can be decomposed locally into two dynamically independent motions: acoustic and vortical modes (Kovasznay 1953). Physically, they correspond to sound waves (of infinite wavelength) and vorticity fluctuation, respectively. The latter is convected by the free stream and is often referred to as a convecting gust. The length and time scales of each mode do not match with those of T-S waves simultaneously. Thus, in order for them to excite any T-S wave, a scale-conversion mechanism is required.

As was first explained by Goldstein (1983), the relevant scale-conversion may be achieved by the leading-edge adjustment, where an unsteady perturbation interacts with the non-parallel mean flow near the leading edge to excite the so-called Lam–Rott eigensolution, which then undergoes wavelength shortening and finally evolves into a T-S wave near the lower branch of the neutral stability curve. Another scale-conversion process involves scattering of an acoustic disturbance by localized inhomogeneity, such as a rapidly varying mean flow induced by an isolated roughness

or a sudden change in surface curvature, as was elucidated in the seminar work of Goldstein (1985) and Ruban (1984). Duck, Ruban & Zhikharev (1996) show that a similar process operates for a vortical disturbance to generate T-S waves (see below). This process is commonly referred to as local acoustic (vortical) receptivity. Wu (1999) pointed out that a mutual interaction between a sound wave and a convecting gust with suitable frequencies can also lead to scale-conversion, thereby generating a T-S wave without the involvement of roughness.

The relative importance of these receptive mechanisms depends on the particular situation involved, e.g. the degree of the local inhomogeneity. In the case where the inhomogeneity arises at the junction between a leading-edge ellipse and the flat portion of the plate, the leading-edge receptivity and the local acoustic receptivity are of equal importance (Wanderley & Corke 2001).

The present work is concerned with local vortical receptivity. It is promoted by the recent experiments of Dietz (1999), in which the vortical perturbation was introduced in a controlled manner for the first time. Using a vibrating ribbon in the oncoming free steam, he successfully generated a single-frequency vortical disturbance, a convecting wake. His experiments provided the much needed quantitative data about the amplitude of the T-S waves excited by this receptivity mechanism.

Previously, the receptivity process to a vortical disturbance was formulated and analysed by Kerschen (1991) and Duck, *et al.* (1996), using the high-Reynolds-number approach, i.e. triple-deck theory. The physics and mathematics involved are somewhat similar to those in the acoustic receptivity due to a sound wave interacting with an isolated roughness (cf. Ruban 1984; Goldstein 1985). The main difference is that a vortical disturbance does not penetrate into the boundary layer. Instead it is largely 'absorbed' by the so-called edge layer centred at the outer reach of the boundary layer As a consequence, the dominant interaction occurs in the upper deck (and also in the edge layer) rather than in the lower deck. The coupling coefficient, which measures receptivity effectiveness, is found to be a factor $R^{-1/8}$ smaller than that for the corresponding acoustic case, where R is the global Reynolds number based on the distance of the roughness to the leading edge. Duck *et al.* (1996) derived an explicit formula that approximates the amplitude of the T-S waves to leading order. Kerschen gave no final analytical result, but presented some numerical results to illustrate the efficiency function. On the other hand, Choudhari (1996) studied the same kind of interaction between a three-dimensional gust and a localized roughness using a finite-Reynolds-number approach based on the Orr–Sommerfeld (O-S) equation. His theoretical results provided an important guide for Dietz's experiments.

Dietz (1999) compared his experimental data with the calculations of Choudhari (1996). The latter was found to under-predict by about 20%. Nevertheless such an agreement indicates that the basic mechanism proposed in previous theoretical studies is correct. Dietz also made a comparison with the asymptotic results of Kerschen (1991). Somewhat surprisingly, the latter turned out to be just about 40% of the measured values, which is a substantial discrepancy. Clearly, the agreement with either type of theory cannot be regarded as completely satisfactory, and the rather poor prediction by the asymptotic approach is a matter for concern. For these reasons, there remains a degree of hesitation in accepting fully the local vortical receptivity mechanism as set forth in the existing theories. A further study is necessary to resolve these issues.

In the present paper, the asymptotic theory of Kerschen (1991) and Duck *et al.* (1996) will be refined in two aspects. First, the local vortical receptivity will be reformulated to allow for an arbitrary profile of a periodic convecting gust. Secondly,

the asymptotic expansion will be carried out to second order so that the amplitude of the T-S waves can be determined to $O(R^{-1/8})$ accuracy. The main aims are (i) to evaluate the existing theory by a detailed quantitative comparison with the experimental data of Dietz (1999), and (ii) to provide a self-consistent theory that is also quantitatively accurate.

A second-order theory for distributed receptivity was constructed recently by Wu (2001), and the accuracy of the theoretical predictions was found to be satisfactory. There is now a consensus that triple-deck theory is able to predict receptivity with considerable reliability even though it is inaccurate in describing the neutral stability curve at moderate Reynolds numbers (see e.g. Choudhari & Streett 1992). In addition to being necessary for maintaining self-consistency, triple deck formalism allows the analysis to proceed without prescribing a specific normal distribution of the vortical perturbation. The final answer can be expressed in relatively simple form. Therefore, the present approach will offer considerable analytical insight into the problem.

It should be remarked that the literature on boundary-layer receptivity is extensive. Earlier work in the subject was reviewed by Goldstein & Hultgren (1989), whereas surveys of more recent developments can be found in Choudhari (1993, 1998) and Wu (1999, 2001). References to Russian literature on this subject can be found in Kozlov & Ryzhov (1990) and Duck *et al.* (1996). For the latest contributions to the receptivity of parabolic and elliptic leading edge to acoustic disturbances, the reader is referred to Wanderley & Corke (2001) and references therein. There has also been much work on the receptivity of three-dimensional and supersonic boundary layers (see e.g. Ng & Crouch 1999; Maslov *et al.* 2001).

The rest of the paper is organized as follows. In § 2, we formulate the problem in the framework of the high-Reynolds-number approach. Appropriate scalings are introduced and the vortical perturbation in the oncoming flow is described. This is followed by consideration of the mean-flow distortion induced by a localized roughness, whose height is assumed to be sufficiently small to allow for a linearized analysis. The solution is obtained up to $O(R^{-1/8})$ by using the Fourier transform. In § 3, we investigate the receptivity due to the interaction between a convecting gust and the mean-flow distortion, which takes place in the upper deck as well as in the edge layer. These two regions are analysed in § 3.1 and 3.2, respectively. The main deck acts to facilitate the pressure–displacement interplay between the upper and lower decks as in the standard triple deck, and the solution is given in § 3.3. The forcing from the upper and edge layers is transmitted to the lower deck and results in inhomogeneous systems, which are solved to obtain the unsteady response to the forcing in the Fourier space. The excited T-S wave corresponds to the residue of the Fourier inversion integral, which is evaluated in § 4 to obtain a second-order approximation for the amplitude. We show that in certain conditions, the receptivity is independent of the vertical structure of the gust. An appropriate efficiency function is defined to quantify the receptivity. Numerical calculations are presented in § 5. The theoretical results are compared with the experiments of Dietz (1999) as well as with the relevant previous calculations. It is also shown how the receptivity due to multiple roughness elements can be predicted by an appropriate superposition of the contribution from each element. Some concluding remarks are given in § 6.

2. Formulation and scalings

We consider the two-dimensional incompressible boundary layer over a semi-infinite flat plate, with a localized two-dimensional roughness at a distance L downstream

from the leading edge. The oncoming flow is assumed to be uniform with velocity U_∞, perturbed by a two-dimensional small-amplitude vortical disturbance, which will be specified shortly. As usual, the Reynolds number is defined as

$$R = U_\infty L/\nu, \tag{2.1}$$

and we assume that $R \gg 1$, where ν is the kinematic viscosity.

The flow is to be described in the Cartesian coordinate system (x, y) with its origin at the centre of the roughness, where x and y are along and normal to the plate; they are non-dimensionalized by L and $LR^{-1/2}$, respectively. The time variable t is normalized by L/U_∞. The velocity (u, v) is non-dimensionalized by U_∞, while the non-dimensional pressure p is introduced by writing the dimensional pressure as $(p_\infty + \rho U_\infty^2 p)$, where p_∞ is a constant and ρ the fluid density.

The mean flow is the Blasius boundary layer, the profile of which is $U_B(y)$. As $y \to 0$,

$$U_B(y) \to \lambda y,$$

where the skin friction

$$\lambda(x) = \chi(1 + x)^{-1/2} \quad \text{with} \quad \chi \approx 0.332. \tag{2.2}$$

For large Reynolds numbers $R \gg 1$, the frequency $\hat{\omega}_{TS}$ and wavenumber $\hat{\alpha}_{TS}$ of a lower-branch T-S wave scale with R as (Smith 1979)

$$\hat{\omega}_{TS} = R^{2/8}\omega, \quad \hat{\alpha}_{TS} = R^{3/8}\alpha.$$

It is convenient to introduce the faster variables

$$\bar{t} = R^{2/8}t, \quad \bar{x} = R^{3/8}x, \tag{2.3}$$

and a small parameter

$$\epsilon = R^{-1/8}.$$

2.1. *Unsteady vortical disturbance*

In general, the vortical perturbation in the oncoming flow is random in nature and must be represented as a (stochastic) Fourier integral. For simplicity, in the present study we consider the simplest situation where the gust consists of only one Fourier component with a frequency $\hat{\omega}_c$. This assumption is not too restrictive for the intended comparison with Dietz's (1999) experimental data since the gust introduced in his experiments is of such a simple form. In order for the gust to generate T-S waves, $\hat{\omega}_c$ should scale as

$$\hat{\omega}_c = \hat{\omega}_{TS} = R^{2/8}\omega.$$

The velocity field of the gust can be expressed as $\epsilon_c \boldsymbol{u}_c \equiv \epsilon_c(u_c, \epsilon v_c)$, where

$$\boldsymbol{u}_c = \bar{\boldsymbol{u}}_c(\bar{y})\mathrm{e}^{\mathrm{i}(\epsilon\alpha_c\bar{x} - \omega\bar{t})} + \text{c.c.}, \tag{2.4}$$

with ϵ_c and α_c denoting the magnitude and (scaled) wavenumber of the gust, respectively, and $\bar{y}$ being the transverse variable in the upper deck,

$$\bar{y} = \epsilon y.$$

It is worth mentioning that (2.4) is only a reasonable local representation of the gust in the vicinity of the roughness. Over a very long streamwise scale, the viscous attenuation of the gust must be taken into account. Therefore, ϵ_c must be understood

to be the local magnitude of the gust at the site of the roughness. For a small-amplitude gust ($\epsilon_c \ll 1$), its phase speed equals the free-stream velocity, implying that

$$\alpha_c = \omega.$$

The identity of α_c will be retained for book-keeping purpose. As in Wu (2001), the vertical variation of the gust is assumed to occur on the upper-deck variable, much faster than was assumed in Duck *et al.* (1996). For the specific purpose of calculating the gust/mean-flow interaction, the present scaling results in a somewhat more general setting, from which the case considered by Duck *et al.* can be recovered by taking a suitable limit (see § 4).

The specification of a realistic distribution $\bar{\boldsymbol{u}}_c$ has been one of the obstacles in studying the receptivity to vortical disturbances. The experiments of Dietz (1999), in which the gust is a convecting wake, show that provided the centre of the wake is far away from the plate, the detailed structure of $\bar{\boldsymbol{u}}_c$ becomes irrelevant. As far as the receptivity is concerned, the only relevant parameter that characterizes the wake is the 'slip velocity', the streamwise velocity at the outer edge of the boundary layer. We shall provide mathematical evidence to support this conclusion, which is important as it will enable us to circumvent the difficulty mentioned above. In the following, our analysis will proceed for an arbitrary $\bar{\boldsymbol{u}}_c$, assuming only that the vertical component $\bar{v}_c \to 0$ as $\bar{y} \to 0$.

2.2. *The mean-flow distortion*

As far as the receptivity is concerned, the relevant roughness must have a streamwise length scale of order $R^{-3/8}L$, comparable with the wavelength of the T-S wave. Its dimensional height h^* is of $O(R^{-5/8}L)$ or smaller, so triple-deck theory is applicable. We write

$$h^*/L = R^{-5/8}h,$$

with $h = O(1)$ or smaller. The shape of the roughness is given by

$$y = R^{-1/8}hF(\bar{x}). \tag{2.5}$$

Since Dietz's (1999) experiments were conducted in the regime in which the receptivity has a linear dependence on both the roughness height and the magnitude of the vortical disturbance, it is appropriate to assume that the mean-flow distortion and the vortical disturbance are both of sufficiently small magnitude that their self-nonlinearities can be ignored. Formally, this requires that

$$h \ll R^{-1/8}, \quad \epsilon_c \ll R^{-1/8}. \tag{2.6}$$

Since the mean-flow distortion is governed by the linear triple-deck system, its solution can be obtained analytically by using a Fourier transform with respect to $\bar{x}$ (Smith 1973). Let $\hat{F}_w(k)$ denote the Fourier transform of $F_w(\bar{x})$, i.e.

$$\hat{F}_w(k) = \int_{-\infty}^{\infty} F_w(\bar{x})\mathrm{e}^{-\mathrm{i}k\bar{x}}\mathrm{d}\bar{x}.$$

For the purpose of calculating the initial amplitude of the excited T-S wave, only the Fourier transform is needed. We shall therefore present the mean-flow solution in the Fourier spectral space.

In order to develop a second-order asymptotic theory which can predict the initial amplitude of the T-S wave with $O(R^{-1/8})$ accuracy, the mean-flow solution has to be worked out to the same order of accuracy.

In the upper deck, where $\bar{y} = R^{-1/8}y = O(1)$, the steady-flow distortion can be written as $\epsilon^2 h(\boldsymbol{u}_M, p_M) = \epsilon^2 h(u_M, v_M, p_M)$, and the Fourier transform of (u_M, v_M, p_M) has the expansion

$$(\bar{u}_M, \bar{v}_M, \bar{p}_M) = \left(\bar{u}_M^{(1)}, \bar{v}_M^{(1)}, \bar{p}_M^{(1)}\right) + \epsilon\left(\bar{u}_M^{(2)}, \bar{v}_M^{(2)}, \bar{p}_M^{(2)}\right) + \cdots. \tag{2.7}$$

It can be shown that

$$\bar{p}_M^{(j)} = \bar{P}_M^{(j)} \mathrm{e}^{-\bar{\kappa}\bar{y}}, \quad \bar{v}_M^{(j)} = -\mathrm{i}\frac{\bar{\kappa}}{k} P_M^{(j)} \mathrm{e}^{-\bar{\kappa}\bar{y}} \quad (j = 1, 2),$$

where $\bar{P}_M^{(j)}$ is a function of k, and

$$\bar{\kappa} = [(k + \mathrm{i}0)(k - \mathrm{i}0)]^{1/2}.$$

Here $(k \pm \mathrm{i}0)$ indicates that a small positive/negative quantity has been added to k, and the branch cuts of $(k \pm \mathrm{i}0)^{1/2}$ are taken to be in the lower/upper half-plane.

Expansions in the main and lower decks are of the usual form in triple-deck theory, and the solution procedure is similar to that in Smith (1973) and Wu (2001). The details are omitted since they are of little relevance to the present paper. It suffices to mention that matching the solutions in the three decks yields

$$\bar{P}_M^{(1)} = -k^{-2}(\mathrm{i}k\lambda)^{5/3}\mathrm{Ai}'(0)\hat{F}_w/D(k), \tag{2.8}$$

$$\bar{P}_M^{(2)} = -\frac{k\bar{P}_M^{(1)}}{D(k)}\left\{k^{-3}(\mathrm{i}k\lambda)^{5/3}\mathrm{Ai}'(0)(J_\infty - J_0) + I_2\int_0^\infty \mathrm{Ai}(\zeta)\mathrm{d}\zeta\right\}, \tag{2.9}$$

where $\zeta = (\mathrm{i}k\lambda)^{1/3}Y$, and

$$D(k) = \int_0^\infty \mathrm{Ai}(\zeta)\mathrm{d}\zeta + \frac{(\mathrm{i}k\lambda)^{5/3}}{\bar{\kappa}k^2}\mathrm{Ai}'(0). \tag{2.10}$$

with J_∞ and J_0 being defined by (A3) and (A2), respectively and Ai is the Airy function. To $O(\epsilon)$ accuracy, the normal component of the velocity, $\bar{v}_M$, is given by

$$\bar{v}_M(\bar{y}; k) = \frac{\mathrm{i}(\mathrm{i}k\lambda)^{5/3}\mathrm{Ai}'(0)}{k\bar{\kappa}D(k)}\left\{1 - \frac{\epsilon k}{D(k)}\left[\frac{(\mathrm{i}k\lambda)^{5/3}}{k^3}\mathrm{Ai}'(0)(J_\infty - J_0) + I_2\int_0^\infty \mathrm{Ai}(\zeta)\mathrm{d}\zeta\right]\right\}\hat{F}_w(k)\mathrm{e}^{-\bar{\kappa}\bar{y}}. \tag{2.11}$$

3. Gust-roughness interaction

3.1. *The upper deck and nonlinear interaction*

The gust interacts with the roughness-induced mean-flow distortion to generate an unsteady response, whose velocity and pressure expand as

$$\boldsymbol{u} = \epsilon^2\epsilon_c h(\boldsymbol{u}_1 + \epsilon\boldsymbol{u}_2 + \cdots) + \cdots, \tag{3.1}$$

$$p = \epsilon^2\epsilon_c h(p_1 + \epsilon p_2 + \cdots) + \cdots, \tag{3.2}$$

where a bold letter denotes a vector.

It follows from substitution into the Navier–Stokes equations that

$$\nabla \cdot \boldsymbol{u}_1 = 0. \tag{3.3}$$

$$\frac{\partial}{\partial \bar{x}}\boldsymbol{u}_1 = -\nabla p_1 - (\boldsymbol{u}_M \cdot \nabla)\boldsymbol{u}_c - (\boldsymbol{u}_c \cdot \nabla)\boldsymbol{u}_M, \tag{3.4}$$

where the operator ∇ (and ∇^2 below) are defined with respect to the scaled variables $\bar{x}$ and $\bar{y}$. Equations (3.3)–(3.4) can be reduced to a single equation for the pressure p_1

$$\nabla^2 p_1 = -R_p, \tag{3.5}$$

where

$$R_p = \nabla \cdot \{(\boldsymbol{u}_M \cdot \nabla)\boldsymbol{u}_c + (\boldsymbol{u}_c \cdot \nabla)\boldsymbol{u}_M\}. \tag{3.6}$$

Let $(\bar{\boldsymbol{u}}_j, \bar{p}_j)\mathrm{e}^{-\mathrm{i}\omega\bar{t}}$ be the Fourier transform of $(\boldsymbol{u}_j, p_j)$. The Fourier transform of (3.5) is

$$\left(\frac{\partial^2}{\partial \bar{y}^2} - k^2\right)\bar{p}_1 = -\bar{R}_p,$$

with

$$\bar{R}_p(\bar{y}) = 2(k - \epsilon\alpha_c)\left(\mathrm{i}\bar{u}_c' + 2\mathrm{i}\epsilon\alpha_c\bar{u}_c - \epsilon^2\alpha_c\bar{v}_c\right)\bar{v}_M(\bar{y}\,; k - \epsilon\alpha_c), \tag{3.7}$$

where $\bar{v}_M$ is defined by (2.11). Throughout the rest of this section, unless otherwise indicated, the Fourier transform of the mean-flow distortion is evaluated at $(k - \epsilon\alpha_c)$, even though this argument is often suppressed for brevity. The solution for $\bar{p}_1$ is

$$\bar{p}_1 = P_1\mathrm{e}^{-\bar{\kappa}\bar{y}} - \bar{Q}_p, \tag{3.8}$$

where P_1 is a function of k to be determined, and

$$\bar{Q}_p = \mathrm{e}^{-\bar{\kappa}\bar{y}}\int_0^{\bar{y}} \mathrm{e}^{2\bar{\kappa}\bar{y}_1}\int_\infty^{\bar{y}_1} \bar{R}_p(\bar{y}_2)\mathrm{e}^{-\bar{\kappa}\bar{y}_2}\mathrm{d}\bar{y}_2\mathrm{d}\bar{y}_1. \tag{3.9}$$

By substituting $\bar{p}_1$ into the Fourier transform of the vertical momentum equation in (3.4), it can be shown that

$$\bar{v}_1 = (\mathrm{i}k)^{-1}\Bigg\{ - [\mathrm{i}(k - 2\epsilon\alpha_c)\bar{u}_c - \epsilon(k - 2\epsilon\alpha_c)\bar{v}_c]\bar{v}_M + \bar{\kappa}P_1\mathrm{e}^{-\bar{\kappa}\bar{y}} + \left[\mathrm{e}^{\bar{\kappa}\bar{y}}\int_\infty^{\bar{y}} \bar{R}_p\mathrm{e}^{-\bar{\kappa}\bar{y}_1}\mathrm{d}\bar{y}_1 - \bar{\kappa}\bar{Q}_p\right]\Bigg\}. \tag{3.10}$$

As $\bar{y} \to 0$,

$$\bar{v}_1 \to (\mathrm{i}k)^{-1}(F_1 + \bar{\kappa}P_1) + (\mathrm{i}k)^{-1}\{\mathrm{i}(k - \epsilon\alpha_c)[(k - \epsilon\alpha_c)\bar{u}_c(0) + \bar{u}_c'(0)]\bar{v}_M(0) - k^2P_1\}\bar{y} + \cdots, \tag{3.11}$$

where

$$F_1 = -\mathrm{i}(k - 2\epsilon\alpha_c)\bar{u}_c(0)\bar{v}_M(0) - \int_0^\infty \bar{R}_p(\bar{y})\mathrm{e}^{-\bar{\kappa}\bar{y}}\mathrm{d}\bar{y} \tag{3.12}$$

is the forcing due to the vorticity–roughness interaction in the upper layer.

The pressure p_2 in (3.2) satisfies the homogeneous Laplace equation, and its Fourier transform, $\bar{p}_2$, is found to be

$$\bar{p}_2 = \bar{P}_2\mathrm{e}^{-\bar{\kappa}\bar{y}}.$$

The velocity $\bar{v}_2$ may be found from

$$\mathrm{i}k\bar{v}_2 - \mathrm{i}\omega\bar{v}_1 = -\bar{p}_{2,\bar{y}}. \tag{3.13}$$

By substituting in (3.10) and $\bar{p}_2$, it can be shown that, as $\bar{y} \to 0$,

$$\bar{v}_2 \to -\mathrm{i}\frac{\bar{\kappa}}{k}\bar{P}_2 - \mathrm{i}\frac{\omega}{\bar{\kappa}}P_1 + \frac{\mathrm{i}\omega}{k^2}\left\{\mathrm{i}(k - \epsilon\alpha_c)\bar{u}_c(0)\bar{v}_M(0) + \int_0^\infty \bar{R}_p\mathrm{e}^{-\bar{\kappa}\bar{y}}\mathrm{d}\bar{y}\right\} + \cdots. \tag{3.14}$$

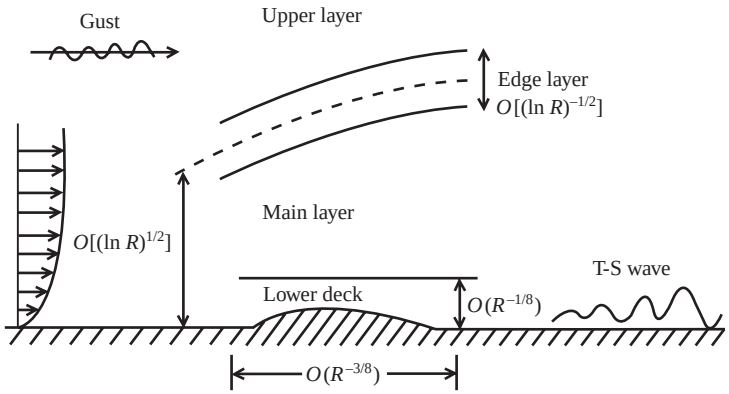

FIGURE 1. Sketch of the receptivity process and the flow structure for the local vortical receptivity.

In contrast to the standard triple-deck, the normal velocity components $\bar{v}_1$ and $\bar{v}_2$ in the upper-deck do not match directly with those in the main deck because of the edge layer sandwiched between them (figure 1). The gust interacts with the mean-flow distortion in this layer to induce a jump in the normal velocity. Duck *et al.* (1996) correctly included the leading-order contribution from this layer by arguing that the streamlines in the upper and main decks should have the same slope (to leading order). In a later paper (Ruban, Duck & Zhikharev 1996), they analysed the edge layer and calculated its contribution. Since it seems impossible to use the argument of Duck *et al.* (1996) to obtain the higher-order contribution, we consider the interaction in the edge layer in some detail in § 3.2.

3.2. *Analysis of the edge-layer interaction*

As was first pointed out by Gulyaev *et al.* (1989), a vortical disturbance is largely 'absorbed' by a relatively thin edge layer sitting on the outer reach of the boundary layer (see figure 1). The Blasius boundary profile there has the approximation

$$U_B \sim 1 - \frac{\hat{a}}{\hat{y} - \hat{b}} \mathrm{e}^{-(1/4)(\hat{y}-\hat{b})^2},$$

where $\hat{y} = y/(1+x)^{1/2}$ is the Blasius similarity variable, $\hat{a} \approx 0.46$ and $\hat{b} \approx 1.72$. The edge layer is centred at $y = (\hat{y}_0 + \hat{b})(1+x)^{1/2} \gg 1$ and has the width $\delta = 2/\hat{y}_0 \ll 1$, where $\hat{y}_0$ is determined by

$$\hat{y}_0^3 \mathrm{e}^{\hat{y}_0^2/4} = 4\hat{a}R^{1/4}, \quad \text{so that} \quad \hat{y}_0 \approx (\log R)^{1/2}.$$

The local transverse variable is defined by

$$\hat{\eta} = (\hat{y} - \hat{y}_b)/\delta \quad \text{with} \quad \hat{y}_b = \hat{y}_0 + \hat{b},$$

and thus $\hat{\eta}$ is related to the upper-deck variable $\bar{y}$ via

$$\bar{y} = \epsilon y = \epsilon(1+x)^{1/2}(\hat{y}_b + \delta\hat{\eta}). \tag{3.15}$$

We now show that the vortical disturbance, while undergoing rapid reduction within the edge layer, interacts with the mean-flow distortion, making a contribution comparable with that from the upper deck to the receptivity. The following analysis is in fact almost the same as in the case of distributed vortical receptivity (Wu 2001), except for some minor differences.

The flow in this region, including the basic Blasius flow, the roughness-induced distortion, the gust as well as the unsteady response to the interaction between the latter two, has the expansion

$$u = [1 - \epsilon^2\delta^{-2}\mathrm{e}^{-\hat{\eta}} + \cdots] + \epsilon^2 h\mathscr{F}^{-1}[\bar{u}_M(0;k) + \cdots] + \epsilon_c[\hat{u}_c(\hat{\eta}) + \epsilon\delta\hat{u}_c^{(1)}(\hat{\eta}) + \cdots]\mathrm{e}^{\mathrm{i}(\epsilon\alpha_c\bar{x}-\omega\bar{t})}$$
$$+\epsilon\delta^{-1}\epsilon_c h[\tilde{u}_1 + \epsilon\tilde{u}_2 + \cdots]\mathrm{e}^{-\mathrm{i}\omega\bar{t}} + \cdots,$$
$$v = \epsilon^2 h\mathscr{F}^{-1}[\bar{v}_M(0;k) + \epsilon\hat{y}_b(1+x)^{1/2}(-\bar{\kappa}\bar{v}_M(0;k)) + \epsilon\delta(-\bar{\kappa}\bar{v}_M(0;k))(1+x)^{1/2}\hat{\eta} + \cdots]$$
$$+\epsilon^2\epsilon_c\delta[\hat{v}_c(\hat{\eta}) + \epsilon\delta\hat{v}_c^{(1)}(\hat{\eta}) + \cdots]\mathrm{e}^{\mathrm{i}(\epsilon\alpha_c\bar{x}-\omega\bar{t})} + \epsilon^2\epsilon_c h[\tilde{v}_1 + \epsilon\tilde{v}_2 + \cdots]\mathrm{e}^{-\mathrm{i}\omega\bar{t}} + \cdots,$$
$$p = \epsilon^2 h\mathscr{F}^{-1}[\bar{p}_M(0;k) + \cdots] + \epsilon^2\epsilon_c h[\tilde{p}_1 + \tilde{p}_2 + \cdots]\mathrm{e}^{-\mathrm{i}\omega\bar{t}} + \cdots,$$

where $\mathscr{F}^{-1}$ stands for the inversion of the Fourier transform. Note that the Fourier transform of the mean-flow distortion in the edge layer is just the Taylor expansion of the corresponding upper-deck solution.

The solution for the gust was first considered by Gulyaev *et al.* (1989), and was developed in more detail by Duck *et al.* (1996). The leading-order terms, $\hat{u}_c$ and $\hat{v}_c$, satisfy

$$\left.\begin{aligned} &\mathrm{i}\alpha_c\hat{u}_c + (1+x)^{-1/2}\hat{v}_c'(\hat{\eta}) = 0, \\ &\hat{u}_c''(\hat{\eta}) + \hat{u}_c' + \mathrm{e}^{-\hat{\eta}}\{\mathrm{i}\alpha_c(1+x)\hat{u}_c - (1+x)^{1/2}\hat{v}_c\} = 0, \end{aligned}\right\} \tag{3.16}$$

subject to the matching conditions with the slip velocity of the gust at the edge of the boundary layer, namely

$$\hat{u}_c \to [\bar{u}_c(0) + \epsilon\hat{y}_b(1+x)^{1/2}\bar{u}_c'(0)], \quad \text{as} \quad \hat{\eta} \to \infty.$$

As was pointed out by Gulyaev *et al.* (1989), the $\hat{u}_c'$ term in (3.16) is associated with thickening of the boundary layer. Thus, in the edge layer, the non-parallelism is a leading-order effect implying that the use of the O-S equation to calculate the signature of the gust is not completely justified.

Eliminating $\hat{u}_c$ between the equations in (3.16) yields

$$\hat{v}_c''' + \hat{v}_c'' + \mathrm{i}\alpha_c(1+x)\mathrm{e}^{-\hat{\eta}}(\hat{v}_c' + \hat{v}_c) = 0.$$

The appropriate solution is (cf. Duck *et al.* 1996)

$$\hat{v}_c = -2\pi\{\alpha_c\bar{u}_c(0) + \epsilon\hat{y}_b(1+x)^{1/2}[\alpha_c\bar{u}_c'(0)]\}(1+x)^{1/2}\hat{\zeta}^2\int_\infty^{\hat{\zeta}}\hat{\zeta}^{-3}H_0^{(1)}(\hat{\zeta})\mathrm{d}\hat{\zeta}, \tag{3.17}$$

where $H_0^{(1)}$ denotes the Hankel function of order zero, and

$$\hat{\zeta} = 2(\mathrm{i}\alpha_c(1+x))^{1/2}\mathrm{e}^{-\hat{\eta}/2}.$$

The exact solutions for $\hat{u}_c^{(1)}$ and $\hat{v}_c^{(1)}$ are not required, and all that we require is that

$$\hat{u}_c^{(1)} \to \bar{u}_c'(0)(1+x)^{1/2}\hat{\eta} \quad \text{as} \quad \hat{\eta} \to \infty, \quad \hat{u}_c^{(1)} \to 0 \quad \text{as} \quad \hat{\eta} \to -\infty.$$

Turn now to the unsteady motion driven by the gust/mean-flow interaction. i.e. the terms $(\tilde{u}_j, \tilde{v}_j, \tilde{p}_j)$ $(j = 1, 2)$. Strictly speaking, $(\tilde{u}_2, \tilde{v}_2)$ should expand as a power series of δ, i.e. $\tilde{u}_2 = \delta^{-1}\tilde{u}_2^{(1)} + \tilde{u}_2^{(2)} + \delta\tilde{u}_2^{(3)} + \cdots$, etc. However, such a formal procedure can be

avoided by tactically retaining the $O(\epsilon\delta^{-1})$ forcing terms in the equation for $(\tilde{u}_1, \tilde{v}_1)$, and the $O(\delta)$ terms in the equations for $(\tilde{u}_2, \tilde{v}_2)$. Let the Fourier transform of $(\tilde{u}_j, \tilde{v}_j, \tilde{p}_j)$ be denoted by $(\hat{u}_j, \hat{v}_j, \hat{p}_j)$. Then the governing equations for $(\hat{u}_j, \hat{v}_j, \hat{p}_j)$ are as follows

$$\mathrm{i}k\hat{u}_1 + (1+x)^{-1/2}\hat{v}_{1,\hat{\eta}} = 0, \tag{3.18}$$

$$\mathrm{i}k\hat{u}_1 = -\{1 - \epsilon(1+x)^{1/2}\hat{y}_b(k - \epsilon\alpha_c)\}(1+x)^{-1/2}\bar{v}_M(0; k - \epsilon\alpha_c)\hat{u}_c'(\hat{\eta}), \tag{3.19}$$

$$\mathrm{i}k\hat{u}_2 + (1+x)^{-1/2}\hat{v}_{2,\hat{\eta}} = 0,$$

$$\mathrm{i}k\hat{u}_2 - \mathrm{i}\omega\hat{u}_1 = -\delta(\mathrm{i}k\bar{P}_1) - \delta(1+x)^{-1/2}\bar{v}_M(0)\hat{u}_{c,\hat{\eta}}^{(1)}$$

$$-\delta(k - \epsilon\alpha_c)[\mathrm{i}\bar{u}_M(0)\hat{u}_c(\hat{\eta}) - \bar{v}_M(0)\hat{\eta}\hat{u}_c'(\hat{\eta})].$$

Here, we have used the fact that $\hat{p}_1 = \bar{P}_1$. These equation can be solved to give

$$\hat{v}_1 = C_1 + [1 - \epsilon(1+x)^{1/2}\hat{y}_b(k - \epsilon\alpha_c)]\bar{v}_M(0)\hat{u}_c(\hat{\eta}), \tag{3.20}$$

$$\hat{v}_2 = C_2 + \frac{\omega}{k}[1 - \epsilon(1+x)^{1/2}\hat{y}_b(k - \epsilon\alpha_c)]\bar{v}_M(0)\hat{u}_c(\hat{\eta}) + \delta(\mathrm{i}k\bar{P}_1)\hat{\eta}(1+x)^{1/2}$$

$$-\delta(k - \epsilon\alpha_c)\bar{v}_M(0)\left[\hat{\eta}\hat{u}_c(\hat{\eta}) - 2\int_{-\infty}^{\hat{\eta}}\hat{u}_c(\hat{\eta})\mathrm{d}\hat{\eta}\right](1+x)^{1/2} + \delta\bar{v}_M(0)\hat{u}_c^{(1)}(\hat{\eta}), \tag{3.21}$$

where C_1 and C_2 are functions of k, to be found by matching with the upper-deck solution. It is straightforward to write down the asymptote of the edge-layer solution $(\hat{v}_1 + \epsilon\hat{v}_2)$ as $\hat{\eta} \to \infty$. On rewriting it in terms of $\bar{y}$ (see (3.15)) and matching with the upper-deck solution given by (3.11) and (3.14), we find that

$$C_1 = (\mathrm{i}k)^{-1}\{F_1 + \bar{\kappa}P_1\} + \{-\bar{u}_c(0)\bar{v}_M(0) + 2\epsilon(1+x)^{1/2}\hat{y}_b(k - \epsilon\alpha_c)\bar{u}_c(0)\bar{v}_M(0)\},$$

$$C_2 = -\mathrm{i}\frac{\bar{\kappa}}{k}\bar{P}_2 - \mathrm{i}\frac{\omega}{\bar{\kappa}}P_1 + \mathrm{i}kP_1(1+x)^{1/2}\hat{y}_b - \frac{\omega}{k}\bar{v}_M(0)\bar{u}_c(0) - 2\delta(k - \epsilon\alpha_c)J_c\bar{v}_M(0)\bar{u}_c(0)$$

$$+\frac{\mathrm{i}\omega}{k^2}\left\{\mathrm{i}(k - \epsilon\alpha_c)\bar{u}_c(0)\bar{v}_M(0) + \int_0^{\infty}\bar{R}_p\mathrm{e}^{-\bar{\kappa}\bar{y}}\mathrm{d}\bar{y}\right\},$$

where

$$J_c = -\left[1 + (2\gamma_E + \log\alpha_c - \tfrac{1}{2}\pi\mathrm{i})\right]$$

with $\gamma_E \approx 0.5772$ being Euler's constant.

3.3. *The main-deck solution*

Since the signature of the gust is exponentially small within the boundary layer, no further interaction takes place there. The motion on the T-S wave scales arises merely as the response to the forcing from the upper and edge layers. The Fourier transform of the solution expands as

$$\hat{u} = \epsilon\epsilon_c h[U_1 + \epsilon U_2 + \cdots]\mathrm{e}^{-\mathrm{i}\omega\bar{t}}, \tag{3.22}$$

$$\hat{v} = \epsilon^2\epsilon_c h[V_1 + \epsilon V_2 + \cdots]\mathrm{e}^{-\mathrm{i}\omega\bar{t}}, \tag{3.23}$$

$$\hat{p} = \epsilon^2\epsilon_c h[P_1 + \epsilon P_2 + \cdots]\mathrm{e}^{-\mathrm{i}\omega\bar{t}}. \tag{3.24}$$

The leading-order streamwise and vertical velocities have the familiar solution

$$U_1 = B_1 U_B', \quad V_1 = -\mathrm{i}kB_1 U_B, \tag{3.25}$$

where B_1 is a function of k.

The second-order terms in the expansion, U_2 and V_2, satisfy

$$\mathrm{i}kU_2 + V_{2,y} = 0, \tag{3.26}$$

$$\mathrm{i}kU_B U_2 + U_B' V_2 = \mathrm{i}\omega U_1 - \mathrm{i}kP_1, \tag{3.27}$$

$$\mathrm{i}kU_B V_1 = -P_{2,y}. \tag{3.28}$$

They are solved, after inserting in (3.25), to give (cf. Ryzhov & Terent'ev 1977; Smith 1979)

$$V_2 = -\mathrm{i}kB_2 U_B + \mathrm{i}\omega B_1 + \mathrm{i}kP_1 U_B \int_{\tilde{a}}^{y} \frac{\mathrm{d}y}{U_B^2}, \tag{3.29}$$

$$P_2 = \tilde{P}_2 - k^2 B_1 \int_0^y U_B^2 \mathrm{d}y, \tag{3.30}$$

where B_2 and $\tilde{P}_2$ are functions of k to be determined later, and $\tilde{a}$ is an arbitrary 'constant'; see the Appendix. It is easy to show that as $y \to \infty$,

$$\left.\begin{aligned} V_2 &\to (\mathrm{i}kP_1)y + (-\mathrm{i}kB_2 + \mathrm{i}\omega B_1 + \mathrm{i}kP_1 J_\infty(x)) + \cdots, \\ P_2 &\to (-k^2 B_1)y + (\tilde{P}_2 - k^2 B_1 I_2(x)) + \cdots, \end{aligned}\right\} \tag{3.31}$$

where $J_\infty(x)$ and $I_2(x)$ are given by (A3) and (A1) respectively.

Now since there is no pressure variation across the edge layer, the pressure in the main deck actually matches directly with that in the upper deck, leading to

$$\bar{P}_2 = \tilde{P}_2 - k^2 B_1 I_2. \tag{3.32}$$

Matching the vertical velocity at $O(\epsilon^2 \epsilon_c h)$ and $O(\epsilon^3 \epsilon_c h)$ with the edge-layer solution gives

$$k^2 B_1 = \bar{\kappa} P_1 + F_v, \tag{3.33}$$

$$-\mathrm{i}kB_2 + \mathrm{i}\omega B_1 + \mathrm{i}kP_1 J_\infty = -\frac{\mathrm{i}\bar{\kappa}}{k}\bar{P}_2 - \mathrm{i}\frac{\omega}{\bar{\kappa}}P_1 + (\mathrm{i}k)^{-1} F_c. \tag{3.34}$$

where

$$F_v(k - \epsilon\alpha_c) = -2\mathrm{i}(k - \epsilon\alpha_c)\bar{v}_M(0; k - \epsilon\alpha_c)\bar{u}_c(0) - \int_0^\infty \bar{R}_p(\bar{y})\mathrm{e}^{-\bar{\kappa}\bar{y}}\mathrm{d}\bar{y}$$
$$+\epsilon(1+x)^{1/2}\hat{y}_b[2\mathrm{i}k(k - \epsilon\alpha_c)]\bar{v}_M(0; k - \epsilon\alpha_c)\bar{u}_c(0) \tag{3.35}$$

is the main forcing that leads to the generation of the T-S wave, and

$$F_c(k) = -\mathrm{i}\omega\bar{v}_M(0; k - \epsilon\alpha_c)\bar{u}_c(0) - 2\mathrm{i}\delta k(k - \epsilon\alpha_c)J_c\bar{v}_M(0; k - \epsilon\alpha_c)\bar{u}_c(0)$$
$$-\frac{\omega}{k}\left\{\mathrm{i}(k - \epsilon\alpha_c)\bar{v}_M(0; k - \epsilon\alpha_c)\bar{u}_c(0) + \int_0^\infty \bar{R}_p \mathrm{e}^{-\bar{\kappa}\bar{y}}\mathrm{d}\bar{y}\right\}. \tag{3.36}$$

The integral term in (3.35) and (3.36) represents the 'bulk contribution' from the upper deck. For later reference, we perform integration by parts in this integral to

obtain

$$\int_0^\infty \bar{R}_p(\bar{y})\mathrm{e}^{-\bar{\kappa}\bar{y}}\mathrm{d}\bar{y} = \frac{2\mathrm{i}(k-\epsilon\alpha_c)\bar{v}_M(0;k-\epsilon\alpha_c)}{k+\bar{\kappa}-\epsilon\alpha_c}\left\{\epsilon[2\alpha_c\bar{u}_c(0)]\right.$$
$$\left.+(k+\bar{\kappa}+\epsilon\alpha_c)\int_0^\infty \bar{u}_c'\mathrm{e}^{-(k+\bar{\kappa}-\epsilon\alpha_c)\bar{y}}\mathrm{d}\bar{y}\right\}+O(\epsilon^2), \tag{3.37}$$

where the $O(\epsilon^2)$ term in the integrand has been legitimately neglected.

3.4. *The lower-deck response*

In the lower deck, where $Y = R^{1/8}y = O(1)$, the mean flow is approximated, to the required order, by $R^{-1/8}\lambda Y$, with the skin friction λ given by (2.2). The Fourier transform of the unsteady response to the interaction in the upper and edge layers expands as

$$\hat{u} = \epsilon\epsilon_c h[\tilde{U}_1+\epsilon\tilde{U}_2+\cdots]\mathrm{e}^{-\mathrm{i}\omega\bar{t}}, \tag{3.38}$$

$$\hat{v} = \epsilon^3\epsilon_c h[\tilde{V}_1+\epsilon\tilde{V}_2+\cdots]\mathrm{e}^{-\mathrm{i}\omega\bar{t}}, \tag{3.39}$$

$$\hat{p} = \epsilon^2\epsilon_c h[\tilde{P}_1+\epsilon\tilde{P}_2+\cdots]\mathrm{e}^{-\mathrm{i}\omega\bar{t}}. \tag{3.40}$$

The leading- and second-order terms satisfy the same set of linearized boundary-layer equations

$$\mathrm{i}k\tilde{U}_j+\tilde{V}_{j,Y}=0, \tag{3.41}$$

$$\mathrm{i}(k\lambda Y-\omega)\tilde{U}_j+\lambda\tilde{V}_j=-\mathrm{i}k\tilde{P}_j+\tilde{U}_{j,YY}\quad(j=1,2), \tag{3.42}$$

where $\tilde{P}_1 = P_1$. This system is subject to the no-slip condition $\tilde{U}_j = \tilde{V}_j = 0$ on the wall ($Y = 0$), which leads to

$$\tilde{U}_{j,YY}(0) = \mathrm{i}k\tilde{P}_j, \tag{3.43}$$

after setting $Y = 0$ in (3.42). The matching conditions with the main deck are slightly different, namely, as $Y \to \infty$,

$$\tilde{U}_1 \to \lambda B_1, \quad \tilde{U}_2 \to \lambda B_2+\lambda J_0 P_1, \quad Y\to\infty. \tag{3.44}$$

After elimination of the pressure from (3.41)–(3.42), it follows that $\tilde{U}_{j,Y}$ satisfies

$$\left\{\frac{\partial^2}{\partial Y^2}-\mathrm{i}(k\lambda Y-\omega)\right\}\tilde{U}_{j,Y}=0, \tag{3.45}$$

which has the solution

$$\tilde{U}_j = q_j(k)\int_{\eta_0}^{\eta}\mathrm{Ai}(\eta)\mathrm{d}\eta, \tag{3.46}$$

where

$$\eta = (\mathrm{i}k\lambda)^{1/3}Y+\eta_0, \quad \eta_0 = -\mathrm{i}\omega(\mathrm{i}k\lambda)^{-2/3}. \tag{3.47}$$

Application of (3.44) and (3.43) together with (3.47) gives

$$q_1\int_{\eta_0}^{\infty}\mathrm{Ai}(\eta)\mathrm{d}\eta = \lambda B_1, \quad (\mathrm{i}k\lambda)^{2/3}q_1\mathrm{Ai}'(\eta_0)=\mathrm{i}kP_1, \tag{3.48}$$

$$q_2\int_{\eta_0}^{\infty}\mathrm{Ai}(\eta)\mathrm{d}\eta = \lambda B_2+\lambda J_0P_1, \quad (\mathrm{i}k\lambda)^{2/3}q_2\mathrm{Ai}'(\eta_0)=\mathrm{i}k\tilde{P}_2. \tag{3.49}$$

Solving $q_1(k)$ and P_1 from (3.33) and (3.48) we obtain

$$q_1(k) = \frac{\lambda F_v(k-\epsilon\alpha_c)}{k^2\Delta(k)}, \quad P_1(k) = \frac{\lambda(\mathrm{i}k\lambda)^{2/3}\mathrm{Ai}'(\eta_0)}{\mathrm{i}k^3\Delta(k)}F_v(k-\epsilon\alpha_c), \tag{3.50}$$

where

$$\Delta(k) = \int_{\eta_0}^{\infty}\mathrm{Ai}(\eta)\mathrm{d}\eta + \frac{(\mathrm{i}k\lambda)^{5/3}}{\bar{\kappa}k^2}\mathrm{Ai}'(\eta_0). \tag{3.51}$$

Similarly, $q_2(k)$ can be solved from (3.32), (3.34) and (3.49)

$$q_2(k) = \frac{\lambda\bar{\kappa}F_v(k-\epsilon\alpha_c)}{k^2\Delta^2(k)}\left\{\frac{2\omega}{k\bar{\kappa}} + (J_\infty - J_0 - I_2)\right\}\int_{\eta_0}^{\infty}\mathrm{Ai}(\eta)\mathrm{d}\eta$$

$$-\frac{\lambda\bar{\kappa}F_v}{k^2\Delta(k)}\left[\frac{\omega}{k\bar{\kappa}} + (J_\infty - J_0)\right] + \frac{\lambda F_c}{k^2\Delta(k)}. \tag{3.52}$$

To compare with the first-order solution of Duck *et al.* (1996), we set $\epsilon = 0$ in F_v and $\bar{v}_M(0)$ (see (3.35) and (2.11)) to obtain

$$F_v = \frac{-2(\mathrm{i}k\lambda)^{5/3}\mathrm{Ai}'(0)}{\bar{\kappa}D(k)}\hat{F}_w(k)\bar{u}_c(0),$$

which is equivalent to their $-2k^2A_0^{**}B$ if we note $B = \bar{u}_c(0)$. Inserting this into P_1 gives a result which is exactly their (5.17)–(5.18).

4. Receptivity: the amplitude of the Tollmien–Schlichting wave

The results in the previous section allow us to calculate the amplitude of the T-S wave. The leading-order approximation has already been given by Duck *et al.* (1996). We now show how the T-S wave can be determined up to $O(\epsilon)$ accuracy.

To be specific, we consider the streamwise velocity in the lower deck. The first two terms of its Fourier transform are given by (3.46). Thus, the solution in the physical space, accurate up to $O(\epsilon)$, is given by

$$\tilde{u} = \frac{\epsilon_c\epsilon h}{2\pi}\int_{-\infty}^{\infty}\left\{[q_1(k) + \epsilon q_2(k)]\int_{\eta_0}^{\eta}\mathrm{Ai}(\eta)\mathrm{d}\eta\right\}\mathrm{e}^{\mathrm{i}(k\bar{x}-\omega\bar{t})}\mathrm{d}k + O(\epsilon^2). \tag{4.1}$$

Equations (3.50) and (3.52) indicate that $q_1(k)$ and $q_2(k)$ have simple and double poles, respectively, at $k = \alpha$ where α is any root of Δ, i.e.

$$\Delta(\alpha) = 0. \tag{4.2}$$

This equation is the leading-order dispersion relation of the T-S waves. It is known that for a given real frequency ω, there exist multiple roots, but only one of them can possibly lie in the lower half-plane. The integration contour that ensures the causality depends on the location of the roots. If all the roots lie in the upper half-plane, the integration contour (4.1) can be taken to be along the real axis. However, if a root lies in the lower half-plane, the contour must be deformed to lie below that root (see e.g. Goldstein 1985). In either case, the T-S wave corresponds to $2\pi\mathrm{i}$ multiplied by the residue of the integrand in (4.1) at $k = \alpha$. We find that

$$\tilde{u}_{TS} = (\epsilon_c\epsilon h)\frac{\mathrm{i}\lambda F_v(\alpha-\epsilon\alpha_c)}{\alpha^2\Delta'(\alpha)}\left\{\tilde{U}_{TS} + \epsilon(\mathrm{i}\alpha\bar{x})q_c\int_{\eta_0}^{\eta}\mathrm{Ai}(\eta)\mathrm{d}\eta\right\}\mathrm{e}^{\mathrm{i}(\alpha\bar{x}-\omega\bar{t})}, \tag{4.3}$$

where

$$\tilde{U}_{TS} = (1+\epsilon q_\infty)\int_{\eta_0}^{\eta} \mathrm{Ai}(\eta)\mathrm{d}\eta + \epsilon \tfrac{1}{3} q_c\left[(\eta - 3\eta_0)\mathrm{Ai}(\eta) + 2\eta_0 \mathrm{Ai}(\eta_0)\right], \tag{4.4}$$

$$q_\infty = \frac{1}{\Delta'(\alpha)}\left\{\left\{\left[\frac{\alpha F_v'(\alpha-\epsilon\alpha_c)}{F_v(\alpha-\epsilon\alpha_c)} - 1 - \frac{\alpha\Delta''(\alpha)}{\Delta'(\alpha)}\right]\Lambda - \frac{4\omega}{\alpha^2}\right\}\int_{\eta_0}^{\infty}\mathrm{Ai}(\eta)\mathrm{d}\eta + \tfrac{2}{3}\Lambda\eta_0\mathrm{Ai}(\eta_0)\right\} + \left[\frac{F_c}{F_v} - \frac{\omega}{\alpha} - \alpha(J_\infty - J_0)\right], \tag{4.5}$$

$$q_c = \frac{\Lambda}{\Delta'(\alpha)}\int_{\eta_0}^{\infty}\mathrm{Ai}(\eta)\mathrm{d}\eta, \tag{4.6}$$

with

$$\Lambda = \frac{2\omega}{\alpha^2} + (J_\infty - J_0 - I_2). \tag{4.7}$$

The presence of the secular term proportional to $\bar{x}$ in (4.3) implies that (4.3) is no longer valid when $\bar{x} = O(R^{1/8})$. In order to interpret this term properly and also to be precise about what the theory can predict, we must consider the subsequent development of the T-S wave. In the secondary phase, the T-S wave is governed by local parallel stability theory, and its solution, the streamwise velocity in the lower deck say, takes the usual WKBJ form

$$u_{TS} = A_I U_{TS}(Y, x; \epsilon)\exp\left\{\mathrm{i}R^{3/8}\int_0^x \alpha_{TS}(x)\mathrm{d}x - \mathrm{i}\omega\bar{t}\right\}, \tag{4.8}$$

where the constant A_I is the (unknown) amplitude, and $U_{TS}(Y, x; \epsilon)$ is the eigenfunction. The complex wavenumber $\alpha_{TS}(x)$ has the expansion (Smith 1979)

$$\alpha_{TS} = \alpha_1(x) + \epsilon\alpha_2(x) + \cdots, \tag{4.9}$$

with α_1, α_2, etc. being determined by an analysis very similar to that in § 3. The leading-order analysis immediately shows that α_1 is a root of $\Delta(\alpha_1) = 0$, with of course λ now standing for the local wall shear, i.e. $\lambda = 0.332(1+x)^{-1/2}$. After carrying on the analysis to the second order, we find that

$$\alpha_2 = \frac{\alpha_1^2}{a}\left\{\frac{2\omega}{\alpha_1^2} + (J_\infty - J_0 - I_2)\right\}\int_{\eta_0}^{\infty}\mathrm{Ai}(\eta)\mathrm{d}\eta, \tag{4.10}$$

where the constant a is defined by

$$a = \tfrac{2}{3}\eta_0\mathrm{Ai}(\eta_0) + 2\int_{\eta_0}^{\infty}\mathrm{Ai}(\eta)\mathrm{d}\eta + \frac{2}{3}\frac{(\mathrm{i}\alpha_1\lambda)^{5/3}}{\alpha_1^3}\left\{\mathrm{Ai}'(\eta_0) - \eta_0^2\mathrm{Ai}(\eta_0)\right\}. \tag{4.11}$$

Obviously, the dependence of α_1 and α_2 on the slow variable x is parametric so that as $x \to 0$, $\alpha_1 \to \alpha$, and

$$u_{TS} \approx A_I U_{TS}(Y, 0; \epsilon)(1 + \epsilon\mathrm{i}\alpha_2\bar{x})\,\mathrm{e}^{\mathrm{i}(\alpha\bar{x} - \omega\bar{t})}. \tag{4.12}$$

Matching the leading-order terms in (4.3) and (4.8) gives

$$u_I \equiv A_I U_{TS}(Y, 0; \epsilon) = (\epsilon_c\epsilon h)\frac{\mathrm{i}\lambda F_v(\alpha - \epsilon\alpha_c)}{\alpha^2\Delta'(\alpha)}\tilde{U}_{TS}. \tag{4.13}$$

It is easy to verify that $a = \alpha\Delta'(\alpha)$, and then it follows from (4.6) and (4.10) that

$$\alpha_2 = \alpha q_c. \tag{4.14}$$

Therefore, to the required order, the terms proportional to $\bar{x}$ in (4.3) and (4.12) match automatically. It now transpires that the secular term in (4.3) is associated with the second-order correction to the dispersion relation of the T-S wave.

Formally, the amplitude of the T-S wave depends on the vertical structure of the gust in the free stream due to the 'bulk contribution' in F_v and F_c, represented by the integral term in (3.35)–(3.36). However, a close examination of this term reveals that such a dependence should be weak. The argument is the same as that for distributed vortical receptivity (Wu 2001). First, if the vertical variation of a gust occurs on the slow variable $\tilde{y} \equiv \epsilon\bar{y}$, then $\bar{u}_c'(\bar{y}) = O(\epsilon)$ and $\bar{R}_p = O(\epsilon)$, implying that the receptivity to leading-order depends only on the slip velocity of the gust $\bar{u}_c(0)$, unaffected by the detailed distribution of the gust. A typical case is that considered by Duck *et al.* (1996). If the gust is further assumed to be 'compact' in the vertical direction and centred at a large distance $\bar{y}_c \gg 1$ from the wall such that $\bar{u}_c$ is nearly uniform away from $\bar{y}_c$, then we may neglect $\bar{u}_c'(0)$ and its higher-order derivatives. The convecting wake in Dietz's (1999) experiments apparently falls into this category. Then by performing repeated integration by parts in the integral on the right-hand side of (3.37), it can be shown that the integral is smaller than ϵ to any power, i.e.

$$\int_0^\infty \bar{R}_p(\bar{y})\mathrm{e}^{-\bar{\kappa}\bar{y}}\,\mathrm{d}\bar{y} \approx \frac{4\epsilon\mathrm{i}\alpha_c(\alpha-\epsilon\alpha_c)}{2\alpha-\epsilon\alpha_c}\bar{u}_c(0)\bar{v}_M(0;\alpha-\epsilon\alpha_c)\ . \tag{4.15}$$

Therefore, F_v and F_c depend only on the slip velocity $\bar{u}_c(0)$; the detailed profile $\bar{u}_c(\bar{y})$ is irrelevant.

In the study of receptivity, it is convenient to introduce the so-called efficiency function Λ_F to measure the effectiveness of receptivity. For the present problem, Λ_F can be defined by writing u_I into (Dietz 1999)

$$u_I = \epsilon_c\bar{u}_c(0)h\hat{F}_w(\alpha_{TS}-\epsilon\alpha_c)\Lambda_F, \tag{4.16}$$

where $\hat{F}_w$ is the Fourier transform of the roughness shape, and Λ_F is independent of the roughness geometry. The equation (4.13), as it stands, does not meet this requirement because $\tilde{U}_{TS}$ depends on F_v and hence on $\hat{F}_w$; see (4.4) and (4.5). However, on using the relation (4.14), we may write (4.13) as

$$u_I = (\epsilon_c\epsilon h)\frac{\mathrm{i}\lambda F_v(\alpha_1+\epsilon\alpha_2-\epsilon\alpha_c)}{\alpha^2\Delta'(\alpha)} \times\left\{(1+\epsilon q_N)\int_{\eta_0}^{\eta}\mathrm{Ai}(\eta)\,\mathrm{d}\eta+\epsilon\tfrac{1}{3}q_c[(\eta-3\eta_0)\mathrm{Ai}(\eta)+2\eta_0\mathrm{Ai}(\eta_0)]\right\}, \tag{4.17}$$

where

$$q_N = \frac{1}{\Delta'(\alpha)}\left\{-\left\{\left(1+\frac{\alpha\Delta''(\alpha)}{\Delta'(\alpha)}\right)\Lambda-\frac{4\omega}{\alpha^2}\right\}\int_{\eta_0}^{\infty}\mathrm{Ai}(\eta)\mathrm{d}\eta+\tfrac{2}{3}\Lambda\eta_0\mathrm{Ai}(\eta_0)\right\} + \left[\frac{F_c}{F_v}-\frac{\omega}{\alpha}-\alpha(J_\infty-J_0)\right]. \tag{4.18}$$

Equations (3.35), (3.36), (2.11), (3.7) and (4.9) indicate that $F_v(\alpha_1+\epsilon\alpha_2-\epsilon\alpha_c)$ and $F_c(\alpha_1+\epsilon\alpha_2-\epsilon\alpha_c)$ are proportional to $\hat{F}_w(\alpha_{TS}-\epsilon\alpha_c)$, and thus (4.17) is now in the form of (4.16), from which Λ_F can be calculated,

$$\Lambda_F = \frac{\max|u_I|}{\epsilon_c\bar{u}_c(0)h\hat{F}_w(\alpha_{TS}-\epsilon\alpha_c)}. \tag{4.19}$$

In experiments on localized receptivity such as the case studied here, it is usually necessary to measure the streamwise velocity of the T-S wave at some distance downstream, where the wave has attained a sizeable magnitude. That velocity is then extrapolated back to give the velocity at the location of forcing. As (4.8) indicates, the u_I given by (4.17) represents exactly this extrapolated velocity rather than the physical velocity measured directly at the centre of the roughness.

Equation (4.17) along with (4.18) determines the initial amplitude of the T-S wave to $O(\epsilon)$ accuracy. The present asymptotic approach has the advantage that the final result is expressed in a closed form without the need to specify the profile of the vortical perturbation. These results represent an extension of the earlier work of Duck *et al.* (1996).

5. Quantitative results and comparison with experiments

The asymptotic approximation (4.17) for the initial amplitude of the T-S wave is fairly explicit. It can be easily evaluated by computing the Blasius profile and the Airy function $\mathrm{Ai}(\eta)$, using a shooting method based on a fourth-order Runge–Kutta method. The various integrals were evaluated using the trapezoidal rule, or Simpson's rule whenever possible.

To facilitate the comparison with experiments, we normalized the dimensional frequency of the T-S wave, ω^*, as

$$F = \omega^* \nu / U_\infty^2 \times 10^6.$$

which is related to ω, the scaled frequency in the theory, via

$$F = \omega R^{-3/4} \times 10^6. \tag{5.1}$$

In Dietz's (1999) experiments, the slip velocity of the gust is 0.3% of the free-stream velocity, i.e. $\epsilon_c \bar{u}_c(0) = 0.3 \times 10^{-2}$. The wall roughness is modelled by a single strip or an array of strips of polyester tape. Each strip has a dimensional height $h^* = 100\,\mu\mathrm{m}$ and length $2d^* = 25.4\,\mathrm{mm}$.

5.1. *Single roughness element*

Dietz first carried out measurements for a vortical disturbance of a fixed frequency $F = 50$, while an isolated roughness element is positioned at different streamwise locations. The Reynolds number R varies accordingly in the range of 375^2–850^2. We calculated the initial T-S wave amplitude for this set of experiments. In the case of a single strip, the Fourier transform is given by $h\hat{F}_w$ with

$$\hat{F}_w(k) = \frac{\mathrm{i}}{k}(\mathrm{e}^{\mathrm{i}kd} - \mathrm{e}^{-\mathrm{i}kd}), \tag{5.2}$$

where h and d are related to h^* and d^* by the relation

$$h = \epsilon^3 \frac{h^* U_\infty}{\nu} \equiv \epsilon^3 R_h, \quad d = \epsilon^5 \frac{d^* U_\infty}{\nu} \equiv \epsilon^5 R_d, \tag{5.3}$$

with R_h and R_d being the Reynolds numbers based on the roughness height and length, respectively. The skin friction λ involved in (4.17) is assigned its value at the origin $x = 0$.

Consistent with the practice in experimental studies, we use the maximum value of $|u_I|$ as a measure of the T-S wave magnitude. In figure 2, our theoretical results are compared with Dietz' data. The agreement between the second-order theory and the

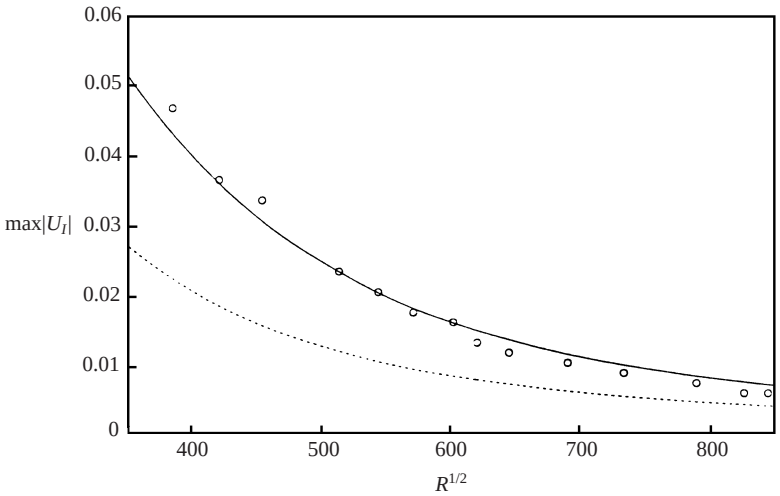

FIGURE 2. Variation of the T-S wave amplitude with the Reynolds number. The frequency of the vortical perturbation $F = 50$. ———, second-order theory; ·····, 'first-order' theory; ○, measurement of Dietz (1999).

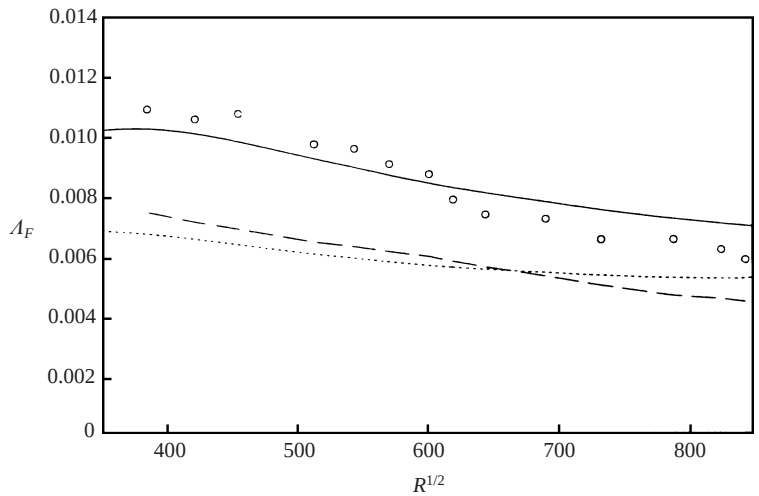

FIGURE 3. Variation of the efficiency function Λ_F with the Reynolds number. ———, second-order theory; ·····, first-order theories; – – – –, finite-Reynolds-number calculations of Choudhari (1996); ○, experiments of Dietz (1999).

experiments is excellent in the whole range of Reynolds numbers. Also included in the figure is the prediction by the 'first-order theory', which is obtained by neglecting all the $O(\epsilon)$ terms in (4.17). The first-order approximation predicts the same trend, but there exists an appreciable error at the low-Reynolds-number end, as is expected. For $R < 600^2$, the typical error is in the range 20%–40%. The first-order theory is sufficiently accurate when $R > 800^2$, indicating that it is capable of capturing the essence of the receptivity process under investigation.

Figure 3 shows the variation of the efficient function Λ_F with the Reynolds number. Again our second-order theory is in good agreement with the experimental data. The first-order result is comparable with the O-S prediction of Choudhari (1996), but both

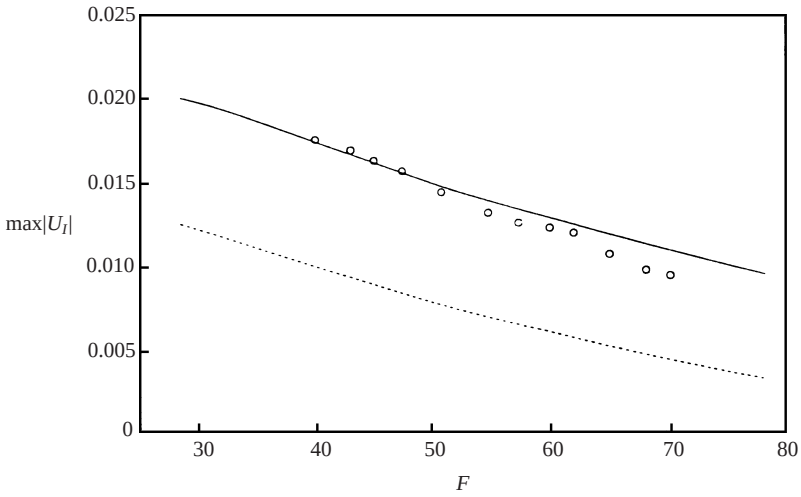

FIGURE 4. Variation of the T-S wave amplitude with the frequency of the vortical perturbation F. The Reynolds number (at the centre of roughness element) $R = 620^2$. ———, second-order theory; · · · · · ·, first-order theory; ○, experiments of Dietz (1999).

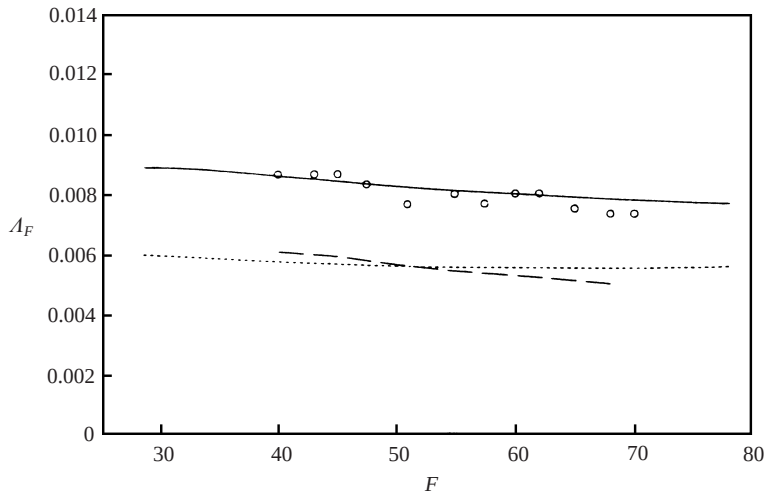

FIGURE 5. Variation of the efficiency function Λ_F with the frequency F. ———, the second-order theory; · · · · · ·, first-order theory; — — —, finite-Reynolds-number result; ○, experiments of Dietz (1999).

underestimate the receptivity by about 30%. We note that the Λ_F predicted by our first-order theory is twice that of Kerschen (1991) quoted in Dietz (1999). This might be because the contribution from the edge layer escaped the attention of Kerschen. This contribution turns out to be identical to that from the upper layer, and thus precisely accounts for the observed difference by a factor of 2.

Dietz (1999) also made detailed measurements with a strip located at a fixed position where the Reynolds number $R = 620^2$, while the frequency of the gust F is varied in the range of 35–70. The T-S wave amplitudes and the efficiency function from our calculations are compared with his data in figures 4 and 5, respectively. Both are predicted accurately by the second-order theory. A marked improvement over both the first-order theory and the finite-Reynolds-number theory is observed.

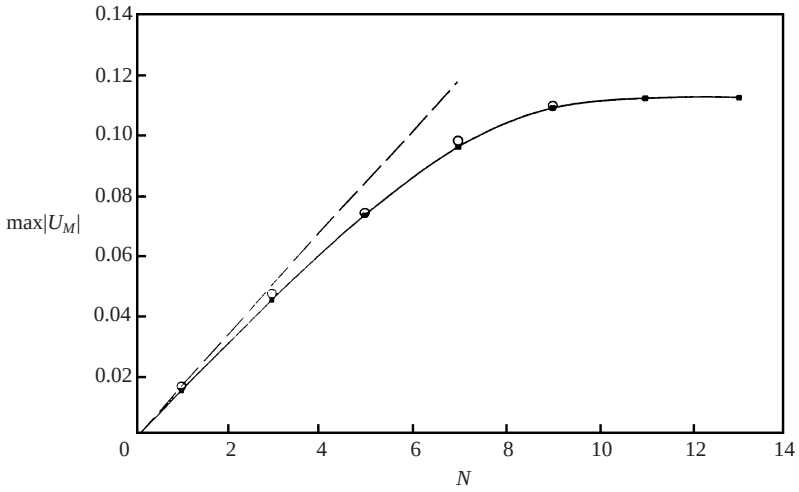

FIGURE 6. Variation of the T-S wave amplitude with the number of roughness elements. The central element is located at the position where $R = 613^2$, and the frequency of the gust $F = 50$. ○, experiments of Dietz (1999); ■, prediction of the second-order theory.

5.2. *Multiple roughness elements*

Dietz (1999) also investigated the case of $N = (2M + 1)$ strips arranged in an array, separated by equal distance l^*. This form of roughness has the Fourier transform

$$\hat{F}_w(k) = \frac{\mathrm{i}}{k}(\mathrm{e}^{\mathrm{i}kd} - \mathrm{e}^{-\mathrm{i}kd}) \sum_{m=-M}^{M} \mathrm{e}^{-\mathrm{i}lkm}, \tag{5.4}$$

where $l = \epsilon^5(l^* U_\infty/\nu) \equiv \epsilon^5 R_l$. Dietz chose $(\alpha_{TS} - \epsilon\alpha_c)l = 2\pi$, for which $\hat{F}_w(\alpha_{TS} - \epsilon\alpha_c) \sim (2M + 1)$. It follows that

$$u_I \sim (2M + 1), \tag{5.5}$$

i.e. the T-S wave amplitude increases linearly with the number of roughness elements. However, such a relation is not expected to hold when N is large. In the strictly asymptotic sense, (5.5) ceases to be valid if $N(2\pi/\alpha_{(TS)}) \sim O(\epsilon^{-3/2})$.

A better viewpoint is to treat each roughness element as independent. At an arbitrary observation position $x \gg x_0$ (with x_0 being the centre of the array), the contribution of the roughness centred at $x_m = ml$ to the T-S wave is

$$u_m \mathrm{e}^{\mathrm{i}\epsilon\alpha_c x_m} \exp\left\{-R^{3/8} \int_{x_m}^{x} \alpha_{TS}(x)\mathrm{d}x\right\},$$

where u_m is the same as u_I provided that the skin friction λ is assigned the local value at $x = x_m$. Superposition of u_m yields the total contribution to the T-S wave

$$\sum_{m=-M}^{M} u_m \mathrm{e}^{\mathrm{i}\epsilon\alpha_c ml} \exp\left\{-R^{3/8} \int_{x_m}^{x} \alpha_{TS}(x)\mathrm{d}x\right\},$$

which is then extrapolated back to obtain the effective T-S wave amplitude at the centre of the array:

$$u_M = \sum_{m=-M}^{M} u_m \mathrm{e}^{\mathrm{i}\epsilon\alpha_c ml} \exp\left\{-R^{3/8} \int_{x_m}^{x_0} \alpha_{TS}(x)\mathrm{d}x\right\}. \tag{5.6}$$

The above formula was used to compute the T-S wave amplitude in the presence of multiple roughness elements. The integrated amplification factor in (5.6) was calculated by using (4.9) and (4.10). In figure 6, the theoretical results are compared with the measurements of Dietz (1999). The prediction is found to have a remarkable accuracy. The linear relation (5.5) gives acceptable approximations for up to 5 elements. However, our theory shows that the T-S amplitude does not increase indefinitely, because the contribution from the elements distant from the centre is exponentially small, as (5.6) indicates. A similar point was made by Choudhari (1993). The receptivity 'saturates' as the number of elements reaches 9, which is exactly what has been observed in the experiments of Dietz. Given that (5.6) is just a superposition of (4.17), it may be stressed that all our theoretical predictions were based on the single formula (4.17).

6. Conclusions

In this paper, we have developed a complete self-consistent second-order asymptotic theory for the receptivity of a boundary layer due to a free-stream vortical perturbation interacting with local roughness. The problem was formulated for an arbitrary profile of the gust, yet the final result can be obtained fairly explicitly, from which it was deduced that the receptivity is largely independent of the normal distribution of the gust.

A comprehensive quantitative comparison has been made with the experimental data of Dietz (1999) as well as with some previous calculations. The first-order theory was found to predict correctly the overall trend of how the receptivity depends on the parameters, but there is appreciable error when the Reynolds number is small. In all cases, the results given by the secondary-order theory were found to be in excellent agreement with measurements. We believe that the present paper has provided sufficient evidence to dispel any uncertainty about the local vortical receptivity mechanism. The second-order asymptotic approximation derived here offers a simple yet quantitatively accurate means for predicting the T-S wave amplitude.

The author would like to thank Professor J. T. Stuart, Professor M. Gaster and Dr M. S. Mughal for helpful discussions. This paper was written up while the author was visiting Tianjin University, China, in January, 2001, and the final revision was made during his sabbatical at the Center for Turbulence Research, Stanford University in July 2001. It is a pleasure to acknowledge the hospitality of these institutions as well as the helpful comments from Professors H. Zhou and J. S. Luo (Tianjin University), and Professors Parviz Moin, Paul A. Durbin, W. C. Reynolds and Sanjiva Lele (Stanford University). Thanks also go to Dr M. E. Goldstein and Dr Meelan Choudhari and the referees for their suggestions and insightful comments.

Appendix. Definition of the integrals

The integrals I_2, J_0 and J_∞ are defined as follows

$$I_2(x) = \int_0^\infty (U_B^2 - 1)\mathrm{d}y, \tag{A1}$$

$$J_0(x) = -\int_0^{\tilde{a}} \left(\frac{1}{U_B^2} - \frac{1}{\lambda^2 y^2}\right)\mathrm{d}y + \frac{1}{\lambda^2 \tilde{a}}, \tag{A2}$$

$$J_\infty(x) = \int_{\tilde{a}}^\infty \left(\frac{1}{U_B^2} - 1\right)\mathrm{d}y - \tilde{a}, \tag{A3}$$

where the parameter $\tilde{a}$ is arbitrary, provided that $\tilde{a} \neq 0$. Since the Blasius profile U_B is a function of the similarity variable $\hat{y} = y/(1+x)^{1/2}$, it is convenient, when evaluating these integrals, to choose $\tilde{a} = \tilde{a}_0(1+x)^{1/2}$ with $\tilde{a}_0$ being independent of x.

REFERENCES

Choudhari, M. 1993 Boundary-layer receptivity due to distributed surface imperfections of a deterministic or random nature. *Theor. Comput. Fluid Dyn.* **4**, 101.

Choudhari, M. 1996 Boundary-layer receptivity to three-dimensional unsteady vortical disturbances in free stream. *AIAA Paper* 96-0181.

Choudhari, M. 1998 Receptivity. In *The Handbook of Fluid Dynamics* (ed. R. W. Johnson), Sect. 13.3, pp. 13-25–13-40. CRC Press.

Choudhari, M. & Streett, C. L. 1992 A finite Reynolds number approach for the prediction of boundary-layer receptivity in localized regions. *Phys. Fluids* **4**, 2495–2514.

Dietz, A. J. 1999 Local boundary-layer receptivity to a convected free-stream disturbance. *J. Fluid Mech.* **378**, 291–317.

Duck, P. W., Ruban, A. I. & Zhikharev, C. N. 1996 Generation of Tollmien–Schlichting waves by free-stream turbulence. *J. Fluid. Mech.* **312**, 341–371.

Goldstein, M. E. 1983 The evolution of Tollmien–Schlichting waves near a leading edge. *J. Fluid Mech.* **127**, 59–81.

Goldstein, M. E. 1985 Scattering of acoustic waves into Tollmien–Schlichting waves by small streamwise variations in surface geometry. *J. Fluid Mech.* **154**, 509–529.

Goldstein, M. E. & Hultgren, L. S. 1989 Boundary layer receptivity to long-wave free-stream turbulence. *Annu. Rev. Fluid Mech.* **21**, 138.

Gulyaev, A. N., Kozlov, V. E., Kuznetson, V. R., Mineev, B. I. & Sekundov, A. N. 1989 Interaction of laminar boundary layer with external turbulence. *Izv. Akad. Nauk SSSR Mekh. Zhid. Gaza.* **6**, 700–710.

Kerschen, E. J. 1991 Linear and nonlinear receptivity to vortical free-stream disturbances. In *Boundary Layer Stability and Turbulence* (ed. D. C. Reda, H. L. Reed & R. K. Kobayashi). ASME FED, vol. 114, 43–48.

Kovasznay, L. S. G. 1953 Turbulence in supersonic flow. *J. Aero. Sci.* **20**, 657–682.

Kozlov, V. V. & Ryzhov, O. S. 1990 Receptivity of boundary layers: asymptotic theory and experiment. *Proc. R. Soc. Lond.* A **429**, 341–373.

Maslov, A. A., Shiplyuk, A. N., Sidorenko, A. A. & Arnal, D. 2001 Leading-edge receptivity of a hypersonic boundary layer on a flat plate. *J. Fluid Mech.* **426**, 73–79.

Morkovin, M. V. 1969 Critical evaluation of transition from laminar to turbulent shear layers with emphasis on hypersonically travelling bodies. US Air Force Flight Dynamics Laboratory, Wright Patterson Air Force Base, Ohio, AFFDL-TR, pp. 68–149.

Ng, L. L. & Crouch, J. D. 1999 Roughness-induced receptivity to crossflow vortices on a swept wing. *Phys. Fluids* A **11**, 432–438.

Reshotko, E. 1976 Boundary layer stability and transition. *Annu. Rev. Fluid Mech.* **8**, 311.

Ruban, A. I. 1984 On Tollmien–Schlichting wave generation by sound. *Izv. Akad. Nauk. SSSR Mekh. Zhid. Gaza* **5**, 44 (in Russian; English Translation: *Fluid Dyn.* **19**, 709–716 (1985)).

Ruban, A. I., Duck, P. W. & Zhikharev, C. N. 1996 The generation of Tollmien–Schlichting waves by free-stream vortical perturbations. *AIAA Paper* 96-2123.

Ryzhov, O. S. & Terent'ev, E. D. 1977 On unsteady boundary layer with self-induced pressure. *Prikl. Mat. Makh.* **41**, 277–301.

Smith, F. T. 1973 Laminar flow over a small hump on flat plate. *J. Fluid Mech.* **57**, 803–824.

Smith, F. T. 1979 On the nonparallel flow stability of the Blasius boundary layer. *Proc. R. Soc. Lond.* A **366**, 91–109.

Wu, X. 1999 Generation of Tollmien–Schlichting waves by convecting gusts interacting with sound. *J. Fluid Mech.* **397**, 285–316.

Wu, X. 2001 Receptivity of boundary layers with distributed roughness to vortical and acoustic disturbances: a second-order asymptotic theory and comparison with experiments. *J. Fluid Mech.* **431**, 91–133.

Wanderley, J. B. V. & Corke, T. C. 2001 Boundary layer receptivity to free-stream sound on elliptic leading edges of flat plates. *J. Fluid Mech.* **429**, 1–21.